

Determination of mechanical properties and thermal treatment behavior of alumina-based refractories

I.D. Katsavou*, M.K. Krokida, I.C. Ziomas

Department of Chemical Engineering, National Technical University of Athens, 9 Iroon Polytechniou str, Zografou Campus, 15780 Athens, Greece

Received 29 February 2012; received in revised form 6 April 2012; accepted 6 April 2012

Available online 15 April 2012

Abstract

Two different types of alumina-based refractories have been investigated. Chamotte and bauxite were the raw materials, being molded using a system of aluminate cement and water or a phenol–formaldehyde resin, as binder. Different raw material's grain size, water content, molding pressure, and firing temperature were selected for the preparation of the specimens. The mechanical strength of all specimens was determined using compressive tests, where parameters with physical meaning, such as maximum stress, maximum strain, elasticity parameter, and viscoelastic parameter were obtained after modeling the collected stress–strain data. In addition, water quenching test was performed for both samples, in order to present their thermal stability and mechanical wear after certain cycles.

Process conditions as well as the raw materials' characteristics were correlated with the compressive properties. More specifically, maximum stress seemed to increase when increasing all parameters except grain size both for bauxite and chamotte samples. The increment of bonding phase, grain size, and molding pressure caused an increment in maximum strain for both types of refractories. However, the higher the firing temperature was the higher the maximum strain of bauxite appeared, while the maximum strain of chamotte samples was decreased. Modulus of elasticity seemed to increase with bonding phase content and firing temperature and decreased with grain size for both types of refractories. For bauxite samples higher molding pressure caused a decrement in elasticity parameter while for chamotte in caused an increment. As far as the quenching tests are concerned chamotte samples seemed to be more tolerant to thermal shock. After data acquisition, the change presented in elasticity parameter (E) was also modeled with the number of cycles. Both bauxite and chamotte samples showed a decrement in maximum stress after thermal treatment, while elasticity parameter seemed to have a more severe decrement for bauxite samples.

© 2012 Elsevier Ltd and Techna Group S.r.l. All rights reserved.

Keywords: Bauxite; Chamotte; Compressive strength; Modeling; Quenching test

1. Introduction

Refractory materials, by definition, are resistant to heat and are exposed to different degrees of mechanical stress and strain, thermal stress etc. [1]. Refractories act as a thermal barrier between a hot medium and the wall of the containing vessel, they insure a strong physical protection, preventing the erosion of walls and they act as thermal insulation, insuring heat retention.

One of the most commonly used raw materials for refractories is bauxite since it appears high bulk density and therefore high compressive strength. Bauxite is an alumina-silica raw material and has the attributes of being relatively inexpensive—at least compared to most basic brick. In addition, they can be used in cases

where modern castable refractories have disadvantages. Chamotte also denotes a mixture of calcined clay and spent ground bricks and it is also used as an inexpensive raw material [2].

One of the most well-known techniques for the production of refractories and ceramics is the mixing of several components in the form of powder, formation of the mixture to the final shape and firing to the suitable temperature, where desired properties are attained [3]. For the formation of refractories different bonding systems can be used, such as ceramic bond, hydraulic bond and organic bond. Ceramic bond is a bond which comes into play typically at high temperatures through ceramization reactions, while hydraulic bond is ensured by the hydration of an aluminous refractory cement added to the product. Finally, in the past decades for the formation of resin bonded refractories phenol–formaldehyde resins are mostly used [4], and are considered as carbonaceous organic binders. The role of the binders is essential in the production of

* Corresponding author. Tel.: +30 210 7723149; fax: +30 210 7723281.

E-mail address: katsavou@central.ntua.gr (I.D. Katsavou).

refractories since they determine the moldability of the product [5] and they ease the transfer of the product from the production line to the kiln, where sintering occurs [3].

Properties such as structural, mechanical and chemical and thermal depend on the type and content of bonding phase, as well as other process conditions, such as molding pressure of the final product, grain size of the raw materials and firing temperature [6,7]. Mechanical properties in room temperature, such as compressive strength and elastic modulus, are essential when selecting refractories and designing refractory components. Therefore, many authors have already examined the mechanical properties of refractories [3,8–11].

On the other hand, thermal shock resistance shows the ability of a structure to withstand rapid changes in temperature with minimal cracking. This situation may occur under conditions when the material is heated or cooled suddenly and it characterizes its thermal profile [1]. One of the common techniques for evaluating thermal shock resistance is the thermal cycling of materials until fracture occurs [12]. Thermal shock tests have been also investigated by many authors [13–15] leading to interesting results for composite materials.

The innovative aspect of this study is the fact that mathematical models were introduced in order to define the mechanical properties in correlation with raw materials' grain size, bonding phase content (resin or water/cement), molding pressure and firing temperature. A number of mathematical models were examined in order to select the most suitable and simple, according to the experimental data [16–18]. The mathematical model for compression involves parameters with physical meaning, such as maximum stress (σ_{\max}), maximum strain (ϵ_{\max}), elasticity parameter (E), and non-linearity parameter (p). On the other hand, thermal shock resistance can be a significant issue, since it causes loss of material due to cracking or even detachment of large sections of the kiln, and is a prospect that should be eliminated. Through this study, selection of optimum conditions for material preparation would be possible in order to result in final products with high strength and toughness, and with the best possible thermal shock resistance.

2. Materials and methods

2.1. Sample preparation

Samples were prepared, using shaft kiln bauxite with particle size from less than 90–315 μm and a phenol formaldehyde resin addition with a content varying from 5

Table 1

Production conditions of tested refractories.

Production conditions					
Bauxite					
Grain size (μm)	90	100	200	315	–
Resin content (%)	0	3	6	10	–
Molding pressure (MPa)	60	100	200	300	400
Firing temperature ($^{\circ}\text{C}$)	1100	1200	1300	1400	–
Chamotte					
Grain size (μm)	200	315	400		
Resin content (%)	5	10	20		
Molding pressure (MPa)	60	100	200		
Firing temperature ($^{\circ}\text{C}$)	1100	1150	1200		

to 10%. In addition, samples using chamotte, having grain sizes varying from less than 200 to 400 μm and water–cement addition with a content varying from 5 to 20% for water and 10% aluminate cement. As grain size it is considered the sieve diameter. The mixing of the raw materials was conducted using a Heidolph RZR 2041 mixer, which ensures uniform mixing. Cylindrical specimens 13 mm in diameter and 14 mm in height where molded applying 60–400 MPa pressure, using a Specac manually operated hydraulic press (25 tn). The bauxite specimens were fired at 1100–1400 $^{\circ}\text{C}$, while the samples produced from the chamotte raw material were fired at 1100–1200 $^{\circ}\text{C}$. Firing at 1100 and 1200 $^{\circ}\text{C}$ was conducted in a Nüve muffle furnace (MF 120), while firing at 1300 and 1400 $^{\circ}\text{C}$ took place in a LECO furnace (model no. 542-500). Table 1 describes the producing conditions thoroughly. All combinations of those parameters were selected, in order to produce samples having different production conditions. For each sample 3 different specimens were fabricated.

2.2. Compression analysis

Compression tests were conducted using an Instron 4482 testing apparatus. Three different specimens for each sample were fitted to the instrument. The uniaxial compression tests were performed at room temperature (25 $^{\circ}\text{C}$). Constant deformation rate of 0.5 mm/min was used for all examined materials and data acquisition was performed in a rate of 4 points/s. Force and deformation were recorded electronically and the resulting stress–strain compression curves were constructed. The compression test was continued until there was a break point of the specimens. Fig. 1 illustrates the specimen before and after the compression test.

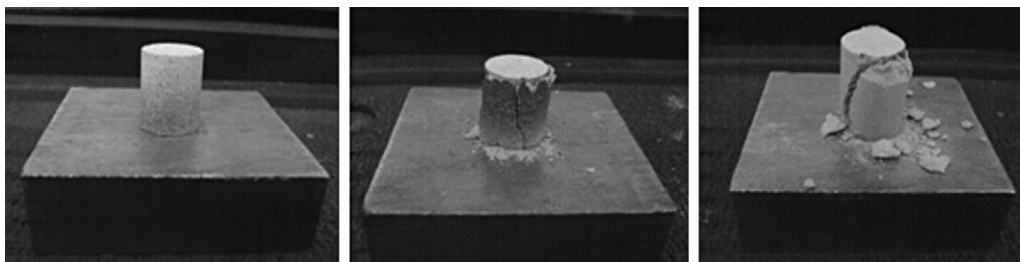


Fig. 1. Specimens before and after compression tests.

2.3. Quenching tests

Thermal shock behavior of the samples was investigated using the water quench test as the experimental method. Samples were cylindrical with a diameter 13 mm and a height of 14 mm. Each thermal shock cycle consisted of several consequent steps. Heating up by a heating speed of 20 °C/min to the quench temperature set at 1200 °C, holding at this temperature for 30 min to reach thermal equilibrium in the whole specimen volume and finally quenching into a water bath at the temperature of 25 °C. This procedure was repeated as many times as required. The water quenching test was applied as an experimental method for thermal stability testing.

3. Mathematical modeling

3.1. Mechanical tests

After data acquisition, the stress–strain equation (Eq. (1)), used in order to present the compression behavior of the samples, involves four parameters: the maximum stress (σ_{\max}), the corresponding strain (ε_{\max}), the elasticity parameter (E) and the non linearity parameter (p) [18,19]. Maximum stress and strain represent the break point of the specimen during compression test. The elasticity parameter represents the linear part of the stress–strain curve and shows the elastic nature of the material. The non linearity exponent represents the exponential part of the curve. This equation was fitted to all data exported from compression tests and the four above mentioned parameters, for each sample, were obtained.

$$\sigma = E \times \varepsilon + (\sigma_{\max} - E \times \varepsilon_{\max}) \times \left(\frac{\varepsilon}{\varepsilon_{\max}} \right)^p \quad (1)$$

Several mathematical models were examined in order to predict the value of stress, strain, elasticity, and viscoelastic parameters against production conditions and materials' characteristics [7,17,18,20]. In order to examine the influence of process characteristics on maximum stress (σ_{\max}), a power

model was used, in which, $\sigma_{\max,0}$ is a multiplication factor, while β_g , β_w/β_r , β_P and β_T are the exponents of grain size, water/resin content, molding pressure and firing temperature, respectively. The proposed model is described by Eq. (2) for bauxite and Eq. (3) for chamotte samples, shown in Table 2.

It is expected that not all of these parameters will influence to the same degree the maximum stress of the products and this may be revealed through regression analysis, by minimizing the following residual sum of squares:

$$S = \left[\frac{\sum_{i=1}^N (\sigma_{\max} - \sigma_{\max}^*)^2}{N - n} \right]^{1/2} \quad (10)$$

where σ_{\max} and σ_{\max}^* are the experimental and the predicted values of maximum stress, respectively, N is the number of experimental points and n is the number of estimated parameters. Following a regression analysis procedure, all the five parameters ($\sigma_{\max,0}$, β_g , β_w/β_r , β_P and β_T) can be determined simultaneously. However, it is not likely that all of these parameters affect the residual sum of squares (S) to the same degree. In order to distinguish between the ones that are necessary for accurately predicting the structural properties, the following procedure was adopted. Firstly, the minimum change in the sum of squares was evaluated for all the five parameters. Secondly, omitting one parameter at a time, the value of σ_{\max} was evaluated for all combinations of the remaining four parameters. In this way, the parameter chosen to be eliminated was the one whose elimination produced the minimum sum of squares. Continuing the former procedure, the minimum sum of squares was evaluated for 4, 3, 2 and 1 parameters, respectively. However, comparing the values of the sum of squares obtained by reducing the number of parameters, there must be an optimum that gives an acceptable accuracy. The same procedure was followed for the estimation of maximum strain, elasticity parameter and non linearity parameter. The exponential models, fitting the experimental data, are also presented in Table 2 and Eqs. (4)–(9). The best value of minimum sum of squares is the one that involves all parameters

Table 2
Mathematical models.

Compression parameters equations

$$\begin{aligned} \sigma_{\max} &= \sigma_{\max,0,1b} \times \left(\frac{g}{g_0} \right)^{\beta_{g1b}} \times \left(\frac{100-r}{100-r_0} \right)^{\beta_{r1b}} \times \left(\frac{P}{P_0} \right)^{\beta_{P1b}} \times \left(\frac{T}{T_0} \right)^{\beta_{T1b}} \\ \varepsilon_{\max} &= \varepsilon_{\max,0,2b} \times \left(\frac{g}{g_0} \right)^{\beta_{g2b}} \times \left(\frac{100-r}{100-r_0} \right)^{\beta_{r2b}} \times \left(\frac{P}{P_0} \right)^{\beta_{P2b}} \times \left(\frac{T}{T_0} \right)^{\beta_{T2b}} \\ E &= E_{\max,0,3b} \times \left(\frac{g}{g_0} \right)^{\beta_{g3b}} \times \left(\frac{100-r}{100-r_0} \right)^{\beta_{r3b}} \times \left(\frac{P}{P_0} \right)^{\beta_{P3b}} \times \left(\frac{T}{T_0} \right)^{\beta_{T3b}} \\ p &= p_{0,4b} \times \left(\frac{g}{g_0} \right)^{\beta_{g4b}} \times \left(\frac{100-r}{100-r_0} \right)^{\beta_{r4b}} \times \left(\frac{P}{P_0} \right)^{\beta_{P4b}} \times \left(\frac{T}{T_0} \right)^{\beta_{T4b}} \end{aligned}$$

$$\begin{aligned} \sigma_{\max} &= \sigma_{\max,0,1c} \times \left(\frac{g}{g_0} \right)^{\beta_{g1c}} \times \left(\frac{100-w}{100-w_0} \right)^{\beta_{w1c}} \times \left(\frac{P}{P_0} \right)^{\beta_{P1c}} \times \left(\frac{T}{T_0} \right)^{\beta_{T1c}} \\ \varepsilon_{\max} &= \varepsilon_{\max,0,2c} \times \left(\frac{g}{g_0} \right)^{\beta_{g2c}} \times \left(\frac{100-w}{100-w_0} \right)^{\beta_{w2c}} \times \left(\frac{P}{P_0} \right)^{\beta_{P2c}} \times \left(\frac{T}{T_0} \right)^{\beta_{T2c}} \\ E &= E_{\max,0,3c} \times \left(\frac{g}{g_0} \right)^{\beta_{g3c}} \times \left(\frac{100-w}{100-w_0} \right)^{\beta_{w3c}} \times \left(\frac{P}{P_0} \right)^{\beta_{P3c}} \times \left(\frac{T}{T_0} \right)^{\beta_{T3c}} \\ p &= p_{0,4c} \times \left(\frac{g}{g_0} \right)^{\beta_{g4c}} \times \left(\frac{100-w}{100-w_0} \right)^{\beta_{w4c}} \times \left(\frac{P}{P_0} \right)^{\beta_{P4c}} \times \left(\frac{T}{T_0} \right)^{\beta_{T4c}} \end{aligned}$$

Parameters

σ_{\max}	Maximum stress	(MPa)	g	Grain size	(μm)
ε_{\max}	Maximum strain	(mm/mm)	w	Water content	(%)
E	Elasticity parameter	(MPa)	r	Resin content	(%)
p	Non linearity parameter	(–)	P	Molding pressure	(MPa)
			T	Firing temperature	(°C)

g_0 , r_0 , w_0 , P_0 , T_0 : constants representing the mean values of g , r , w , P and T , respectively

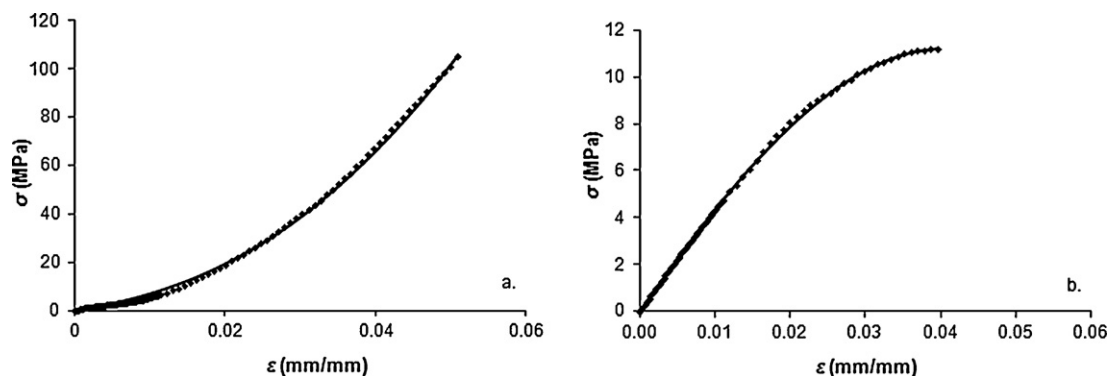


Fig. 2. Indicative stress–strain curves for a. bauxite samples ($g = 315 \mu\text{m}$, $r = 10\%$, $P = 300 \text{ MPa}$, $T_0 = 1400^\circ\text{C}$) and b. chamotte samples ($g = 315 \mu\text{m}$, $w = 20\%$, $P = 300 \text{ MPa}$, $T_0 = 1200^\circ\text{C}$).

Table 3
Results of the parameter estimation for bauxite samples.

Mathematical models	Parameters				
$\sigma_{\max} = \sigma_{\max 0,1b} \times \left(\frac{g}{g_0}\right)^{\beta_{g1b}} \times \left(\frac{100-r}{100-r_0}\right)^{\beta_{r1b}} \times \left(\frac{P}{P_0}\right)^{\beta_{P1b}} \times \left(\frac{T}{T_0}\right)^{\beta_{T1b}}$	$\sigma_{\max 0,1b}$	α_{g1b}	α_{r1b}	α_{P1b}	α_{T1b}
	44.511	−0.372	−3.255	0.381	8.752
$\varepsilon_{\max} = \varepsilon_{\max 0,2b} \times \left(\frac{g}{g_0}\right)^{\beta_{g2b}} \times \left(\frac{100-r}{100-r_0}\right)^{\beta_{r2b}} \times \left(\frac{P}{P_0}\right)^{\beta_{P2b}} \times \left(\frac{T}{T_0}\right)^{\beta_{T2b}}$	$\varepsilon_{\max 0,2b}$	α_{g2b}	α_{r2b}	α_{P2b}	α_{T2b}
	0.034	0.080	−0.217	0.333	1.538
$E = E_{\max 0,3b} \times \left(\frac{g}{g_0}\right)^{\beta_{g3b}} \times \left(\frac{100-r}{100-r_0}\right)^{\beta_{r3b}} \times \left(\frac{P}{P_0}\right)^{\beta_{P3b}} \times \left(\frac{T}{T_0}\right)^{\beta_{T3b}}$	$E_{\max 0,3b}$	α_{g3b}	α_{r3b}	α_{P3b}	α_{T3b}
	559.543	−0.071	−1.426	−0.116	3.328
$p = p_{0,4b} \times \left(\frac{g}{g_0}\right)^{\beta_{g4b}} \times \left(\frac{100-r}{100-r_0}\right)^{\beta_{r4b}} \times \left(\frac{T}{T_0}\right)^{\beta_{T4b}}$	$p_{0,4b}$	α_{g4b}	α_{r4b}		α_{T4b}
	1.962	−0.127	−1.040		1.117

$g_0 = 180 \mu\text{m}$, $r_0 = 4.3\%$, $P_0 = 209 \text{ MPa}$, $T_0 = 1288^\circ\text{C}$

for all the estimated properties except for non linearity parameter, which is not affected by molding pressure.

3.2. Quenching tests

After the thermal shock tests samples were also subjected to mechanical load, in order to measure their maximum stress and their elasticity parameter. The received data (maximum stress and elasticity parameter) were then correlated with the number of cycles using simple polynomial models.

4. Results and discussion

The typical stress–strain curves that were obtained from compression tests and the estimated curves from mathematical model described above (Eq. (1)), for the different materials, are presented in Fig. 2. Accordingly, the corresponding curves referring to different grain sizes, bonding phase contents, molding pressures and firing temperatures were plotted. The bauxite samples present a controlled fracture, typical of a tough material and as alumina is the primary phase and mullite the secondary phase it seems that mullite forms a stiff and interlocked skeleton between α -alumina grains, giving a reinforced effect [10]. As far as chamotte samples are

concerned they appear a break point at lower pressures, having lower strength and low toughness [21].

The values of maximum stress (σ_{\max}), maximum strain (ε_{\max}), the elastic parameter (E), and the viscoelastic parameter (p) were obtained from the stress–strain equation [18]. After regression analysis the parameters of the mathematical models were estimated for bauxite samples, as presented in Table 3.

It was shown that maximum stress increased with all parameter apart from grain size. It is understood that the higher the molding pressure and firing temperatures are the denser the specimens become, as shown in Fig. 3, and therefore the maximum stress increases, which is in accordance with other studies [22,23]. In addition, as it is mentioned in Bonsall's work [24], higher resin content leads to more dense product and therefore samples will withstand higher loads, while low compressive strength corresponds to higher bauxite's grain size [25].

The same dependence of process conditions was shown for maximum strain, except for grain size. Higher grain size seems to lead to higher strain as larger grains can stand more elongation of the sample. The results obtained for maximum strain are presented in Fig. 4.

In Fig. 5, elasticity parameter is presented to be affected proportionally by temperature and resin content, while molding pressure and grain size cause a decrease in E . As an increased

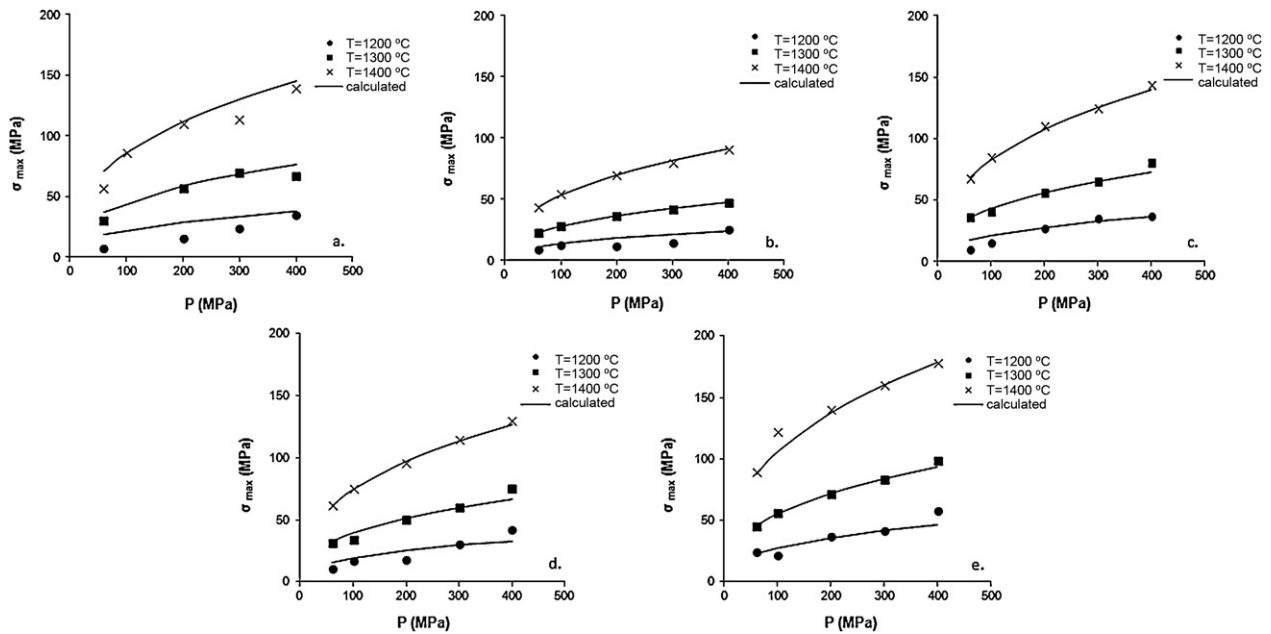


Fig. 3. Effect of molding pressure and firing temperature on maximum stress of bauxite specimens having: (a) $g < 90 \mu\text{m}$ and $r = 3\%$, (b) $200 < g < 315 \mu\text{m}$ and $r = 3\%$, (c) $90 < g < 100 \mu\text{m}$ and $r = 3\%$, (d) $90 < g < 100 \mu\text{m}$ and $r = 0\%$ and (e) $90 < g < 100 \mu\text{m}$ and $r = 10\%$.

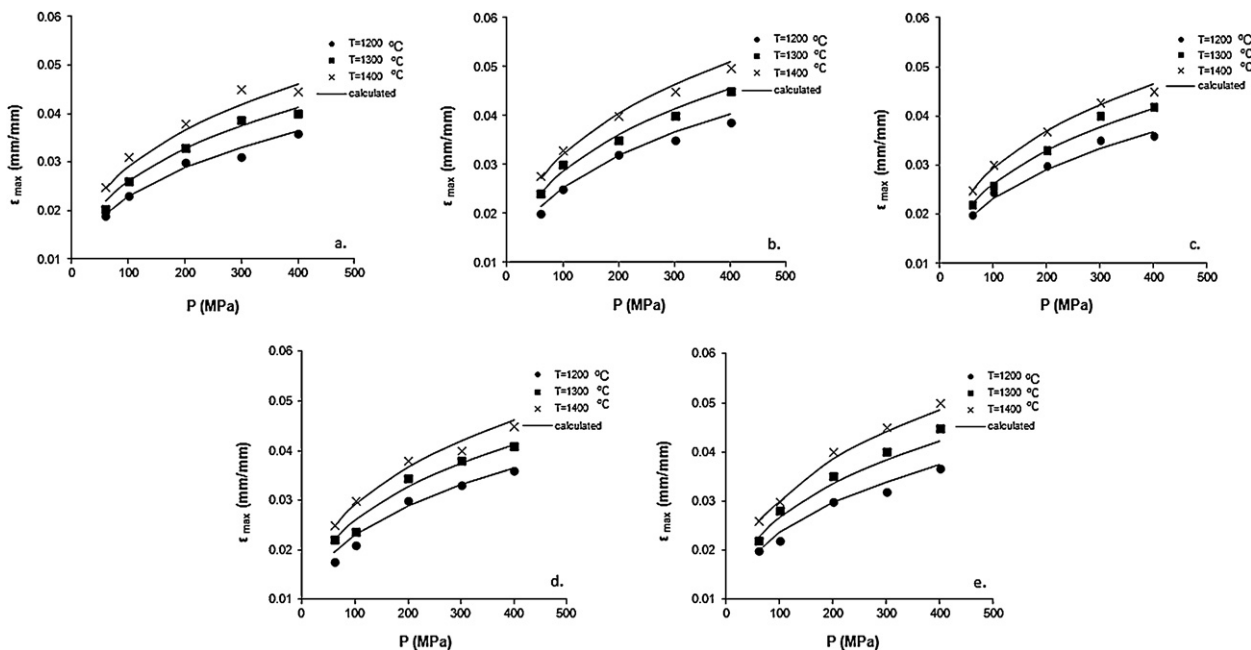


Fig. 4. Effect of molding pressure and firing temperature on maximum strain of bauxite specimens having: (a) $g < 90 \mu\text{m}$ and $r = 3\%$, (b) $200 < g < 315 \mu\text{m}$ and $r = 3\%$, (c) $90 < g < 100 \mu\text{m}$ and $r = 3\%$, (d) $90 < g < 100 \mu\text{m}$ and $r = 0\%$ and (e) $90 < g < 100 \mu\text{m}$ and $r = 10\%$.

elasticity parameter represents stiff materials, it is understood that high grain size will lead to less stiff samples, with less maximum stress as described above [21]. Molding pressure increment also causes a decrement in E because during molding the load influences the elastic deformation of the material [26].

Finally, regression analysis showed that non linearity parameter is not affected by molding pressure. The other process conditions seem to influence p the same way as elastic parameter (Fig. 6).

Table 4 presents the mathematical models and the parameters estimated after regression analysis for chamotte samples.

Maximum stress and elasticity parameter were found to increase with molding pressure, water content, and firing temperature, as indicated in Figs. 7 and 8. The above mentioned process conditions lead to denser specimens as also described for bauxite [19]. The higher amount of water, in addition to the cement bond (10% for all specimens) form

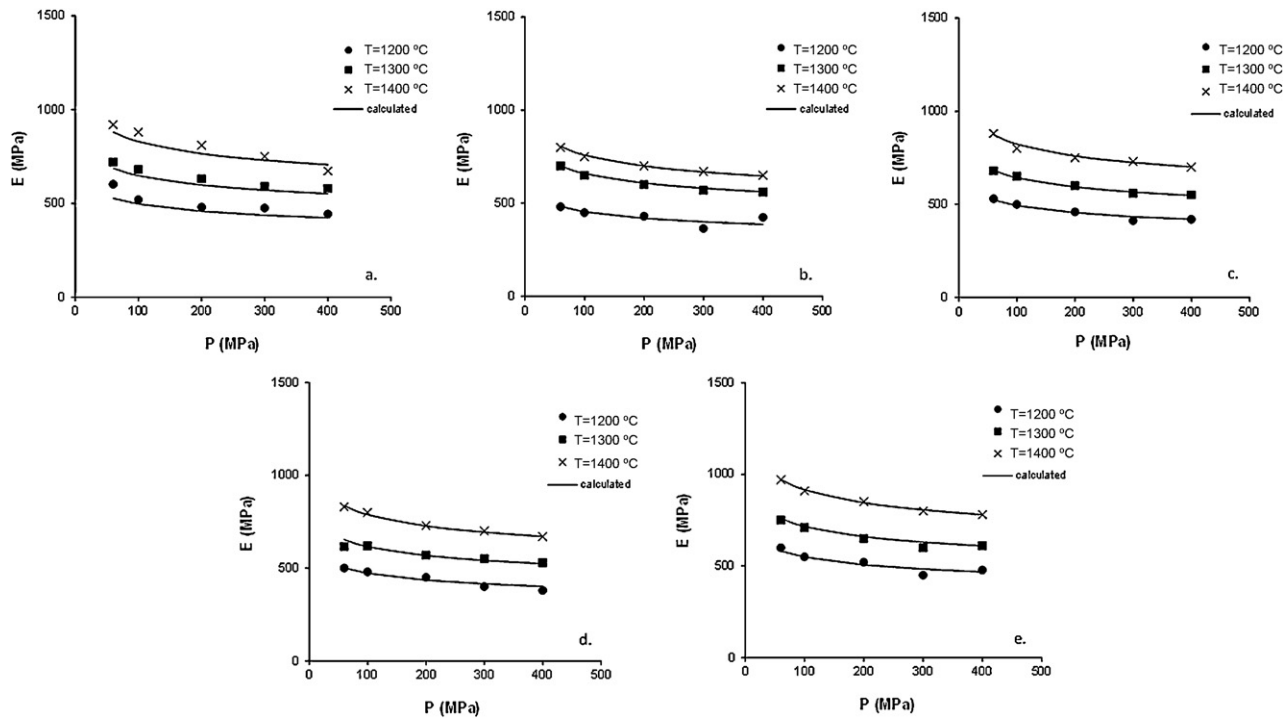


Fig. 5. Effect of molding pressure and firing temperature on elasticity parameter of bauxite specimens having: (a) $g < 90 \mu\text{m}$ and $r = 3\%$, (b) $200 < g < 315 \mu\text{m}$ and $r = 3\%$, (c) $90 < g < 100 \mu\text{m}$ and $r = 3\%$, (d) $90 < g < 100 \mu\text{m}$ and $r = 0\%$ and (e) $90 < g < 100 \mu\text{m}$ and $r = 10\%$.

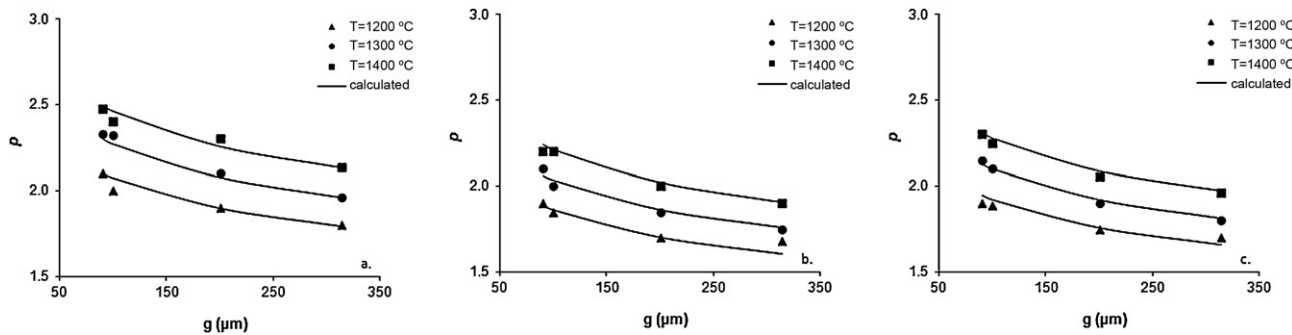


Fig. 6. Effect of grain size and firing temperature on non linearity parameter of bauxite specimens having $P = 100 \text{ MPa}$ and: (a) $r = 10\%$, (b) $r = 0\%$, and (c) $r = 3\%$.

Table 4
Results of the parameter estimation for chamotte samples.

Mathematical models	Parameters				
$\sigma_{\max} = \sigma_{\max 0,1c} \times \left(\frac{g}{g_0}\right)^{\beta_{g1c}} \times \left(\frac{100-w}{100-w_0}\right)^{\beta_{w1c}} \times \left(\frac{P}{P_0}\right)^{\beta_{P1c}} \times \left(\frac{T}{T_0}\right)^{\beta_{T1c}}$	$\sigma_{\max 0,1c}$	β_{g1c}	β_{w1c}	β_{P1c}	β_{T1c}
	6.755	−0.173	−0.875	0.850	9.494
$\varepsilon_{\max} = \varepsilon_{\max 0,2c} \times \left(\frac{g}{g_0}\right)^{\beta_{g2c}} \times \left(\frac{100-w}{100-w_0}\right)^{\beta_{w2c}} \times \left(\frac{P}{P_0}\right)^{\beta_{P2c}} \times \left(\frac{T}{T_0}\right)^{\beta_{T2c}}$	$\varepsilon_{\max 0,2c}$	β_{g2c}	β_{w2c}	β_{P2c}	β_{T2c}
	0.048	0.138	−0.050	0.313	−1.889
$E = E_{\max 0,3c} \times \left(\frac{g}{g_0}\right)^{\beta_{g3c}} \times \left(\frac{100-w}{100-w_0}\right)^{\beta_{w3c}} \times \left(\frac{P}{P_0}\right)^{\beta_{P3c}} \times \left(\frac{T}{T_0}\right)^{\beta_{T3c}}$	$E_{\max 0,3c}$	β_{g3c}	β_{w3c}	β_{P3c}	β_{T3c}
	148.376	−0.378	−1.793	0.123	14.396
$p = p_{0,4c} \times \left(\frac{g}{g_0}\right)^{\beta_{g4c}} \times \left(\frac{100-w}{100-w_0}\right)^{\beta_{w4c}} \times \left(\frac{T}{T_0}\right)^{\beta_{T4c}}$	$p_{0,4c}$	β_{g4c}	β_{w4c}		β_{T4c}
	2.746	0.357	−4.494		5.812

$g_0 = 303 \mu\text{m}$, $r_0 = 12.4\%$, $P_0 = 200 \text{ MPa}$, $T_0 = 1150 \text{ }^\circ\text{C}$

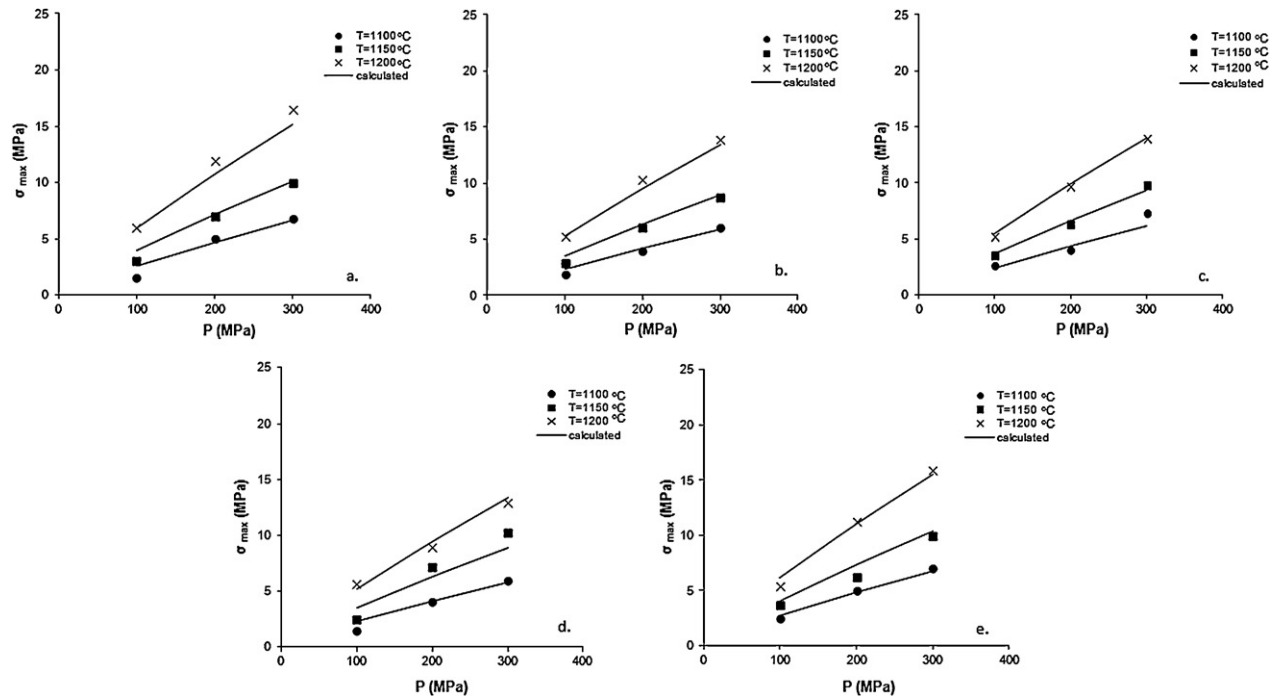


Fig. 7. Effect of molding pressure and firing temperature on maximum stress of chamotte specimens having: (a) $100 < g < 200 \mu\text{m}$ and $w = 10\%$, (b) $315 < g < 400 \mu\text{m}$ and $w = 10\%$, (c) $200 < g < 315 \mu\text{m}$ and $w = 10\%$, (d) $200 < g < 315 \mu\text{m}$ and $w = 5\%$ and (e) $200 < g < 315 \mu\text{m}$ and $w = 20\%$.

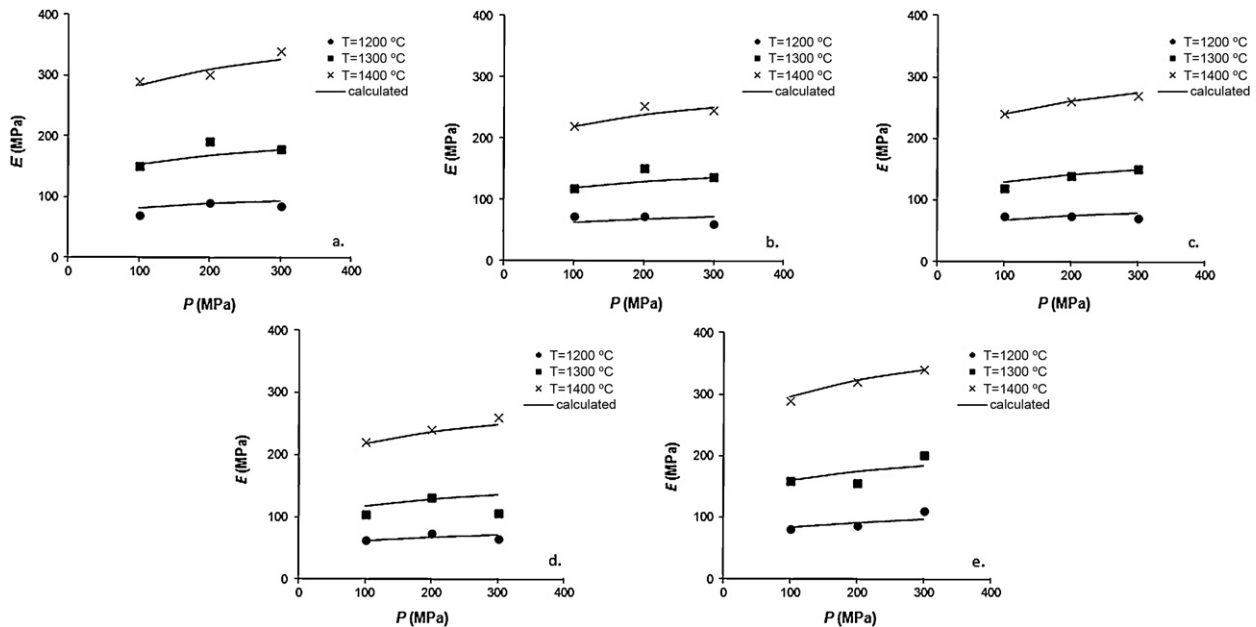


Fig. 8. Effect of molding pressure and firing temperature on elasticity parameter of chamotte specimens having: (a) $100 < g < 200 \mu\text{m}$ and $w = 10\%$, (b) $315 < g < 400 \mu\text{m}$ and $w = 10\%$, (c) $200 < g < 315 \mu\text{m}$ and $w = 10\%$, (d) $200 < g < 315 \mu\text{m}$ and $w = 5\%$ and (e) $200 < g < 315 \mu\text{m}$ and $w = 20\%$.

a stronger hydraulic bond. This bond is ensured by the hydration of the aluminous refractory cement, which is made up of a mixture of calcium aluminates which are hydrated in the presence of water at low temperatures, by provoking hardening of the material [27]. However, grain size seems to reduce both maximum stress and elasticity parameter, as in the case of bauxite samples.

Maximum strain increases with grain size, water content and molding pressure, but it decreases with firing temperature, as

shown in Fig. 9. This phenomenon is explained as the samples become stiffer with increasing the firing temperature the break point occurs in lower elongations. Finally, the non linearity parameter, seems to increase while increasing grain size, water content, and firing temperature and it seems to be independent of molding pressure. The schemes showing the above mentioned tendencies are summarized in Fig. 10.

Quenching tests were conducted in order to determine the minimum shock required to nucleate fracture (cracking), and

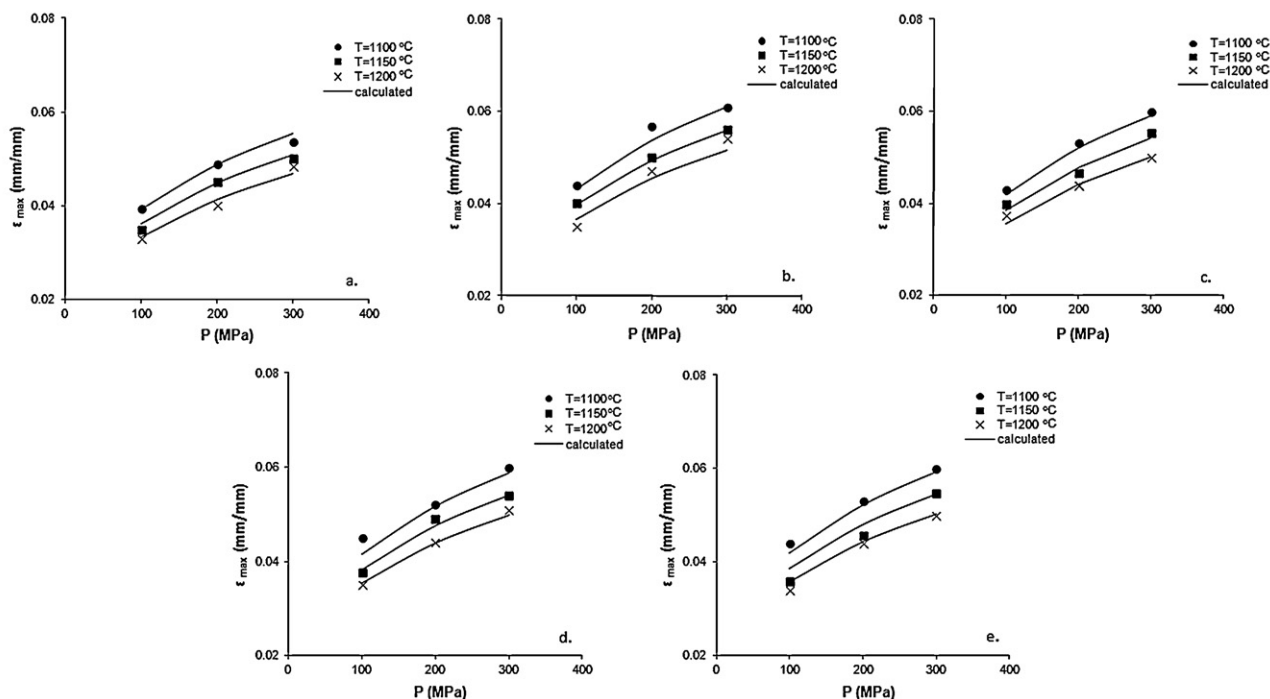


Fig. 9. Effect of molding pressure and firing temperature on maximum strain of chamotte specimens having: (a) $100 < g < 200 \mu\text{m}$ and $w = 10\%$, (b) $315 < g < 400 \mu\text{m}$ and $w = 10\%$, (c) $200 < g < 315 \mu\text{m}$ and $w = 10\%$, (d) $200 < g < 315 \mu\text{m}$ and $w = 5\%$ and (e) $200 < g < 315 \mu\text{m}$ and $w = 20\%$.

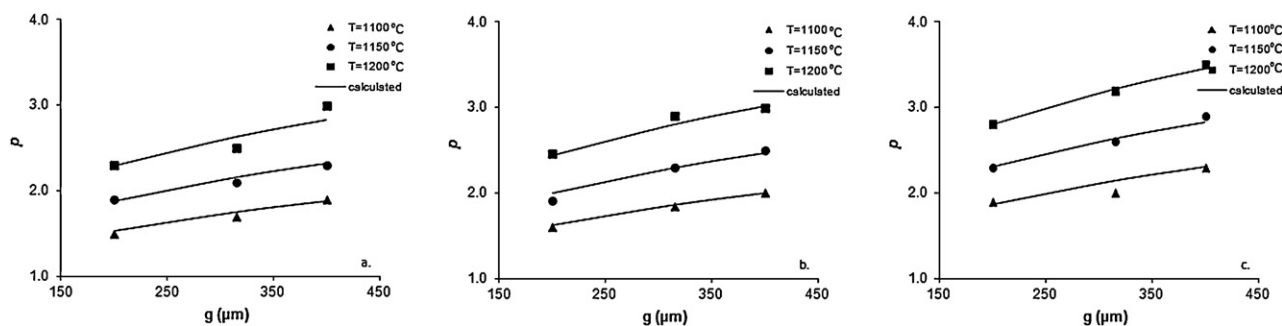


Fig. 10. Effect of grain size and firing temperature on non linearity parameter of chamotte specimens having $P = 100 \text{ MPa}$: (a) $w = 10\%$, (b) $w = 5\%$, and (c) $w = 20\%$.

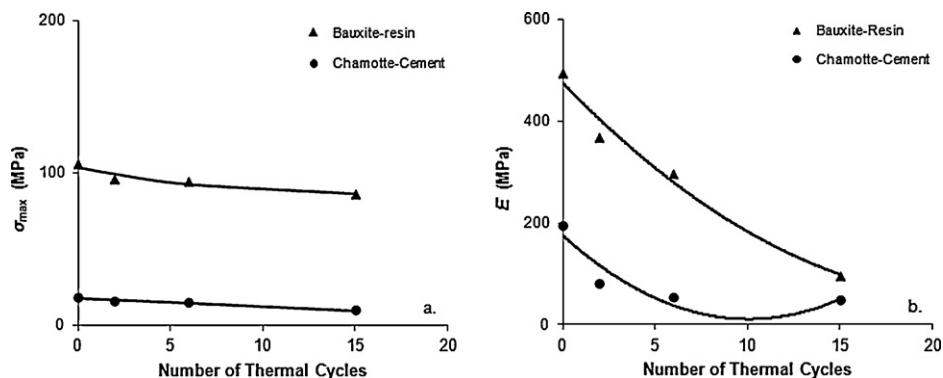


Fig. 11. Graphic presentation of (a) maximum stress and (b) elasticity parameter of samples versus the number of thermal cycles.

the amount of the damage caused by thermal shock [12]. Therefore, after a number of thermal (quenching) cycles, the strength of the materials was compared with the original strength, as well as images, using a stereoscope, were obtained.

In Table 5 the crack propagation can be seen clearly for the bauxite samples, while chamotte samples seem to be more resistant to thermal shock. However, cracks seem to appear in both types of refractories when subjected to quenching. This

Table 5
Specimens during thermal shock.


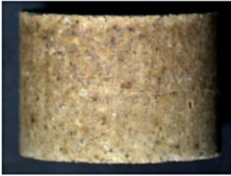
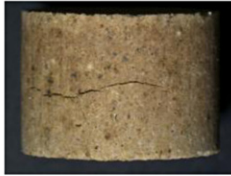





	Before test	After 2 cycles	After 6 cycles	After 15 cycles
Bauxite samples $(g=315\ \mu\text{m},$ $r=10\%,$ $P=300\ \text{MPa},$ $T=1400^\circ\text{C})$				
Chamotte samples $g=315\ \mu\text{m},$ $w=20\%,$ $P=300\ \text{MPa},$ $T=1200^\circ\text{C})$				

Table 6
Mathematical models and parameters' estimation, referring to quenching tests.

Mathematical models	Parameters		
$\sigma_{\max} = \sigma_{0b} \times (\text{cycles})^2 + \sigma_{1b}(\text{cycles}) + \sigma_{2b}$	σ_{0b}	σ_{1b}	σ_{2b}
	0.077	−2.328	103.300
$\sigma_{\max} = \sigma_{0c} \times (\text{cycles})^2 + \sigma_{1c}(\text{cycles}) + \sigma_{2c}$	σ_{0c}	σ_{1c}	σ_{2c}
	−0.003	−0.469	17.405
$E = e_{0b} \times (\text{cycles})^2 + e_{1b}(\text{cycles}) + e_{2b}$	e_{0b}	e_{1b}	e_{2b}
	1.621	−32.651	175.190
$E = e_{0c} \times (\text{cycles})^2 + e_{1c}(\text{cycles}) + e_{2c}$	e_{0c}	e_{1c}	e_{2c}
	0.830	−37.555	475.600

could be caused by defects in the microstructure, resulting either from manufacturing process or nucleated under a thermal loading.

After quenching all specimens were subjected to compression test and the maximum stress and the elasticity parameter were determined, using Eq. (1), as described above. Fig. 11 summarizes the results. More specifically, both bauxite and chamotte samples showed a decrement in maximum stress after thermal treatment, while elasticity parameter seemed to have a more severe decrement for bauxite samples. This can also be confirmed by the stereoscope's images. In these images, it can also be seen that for bauxite samples the cracks began to be obvious after the sixth thermal cycle, while for the chamotte samples cracks appeared at the twelfth cycle, which also strengthens the belief that chamotte samples are more tolerant to thermal shock. The mathematical models describing the above mentioned changes are summarized in Table 6.

5. Conclusions

Maximum stress seemed to increase when increasing all parameters except grain size both for bauxite and chamotte

samples. The increment of bonding phase, grain size, and molding pressure caused an increment in maximum strain for both types of refractories. However, the higher the firing temperature was the higher the maximum strain of bauxite appeared, while the maximum strain of chamotte samples was decreased. Modulus of elasticity seemed to increase with bonding phase content and firing temperature and decreased with grain size for both types of refractories. However, for bauxite samples higher molding pressure caused a decrement in elasticity parameter while for chamotte in caused an increment. Finally, process condition had a positive impact on non linearity parameter apart from grain size which caused an increment in chamotte samples and a decrement in the bauxitic ones.

As far as the quenching tests are concerned chamotte samples seemed to be more tolerant to thermal shock. More specifically, both bauxite and chamotte samples showed a decrement in maximum stress after thermal treatment, while elasticity parameter seemed to have a more severe decrement for bauxite samples, leading to more obvious cracks on the specimens.

References

- [1] C.A. Schacht, Refractories Handbook, Marcel Dekker, N.Y., 2004 p. 499.
- [2] F. Cardarelli, Materials handbook, 2nd ed., Springer, N.Y., 2000, 1364.
- [3] A. Kontopoulos, Introduction to Refractory Materials, N.T.U.A, Athens, 1983, p. 279.
- [4] E. Kagiara, Influence of Resins and Improving Additives on the Alumina-Graphite Refractories' Microstructure and Properties, N.T.U.A, Athens, 1993, p. 307.
- [5] O. Borisenko, G. Semchenko, M. Chirkina, I. Kasymova, High-strength periclase-carbon refractories based on phenol-formaldehyde resin with modification of different batch components, Refractories and Industrial Ceramics 47 (2006) 225–227.
- [6] I.D. Katsavou, M.K. Krokida, I.C. Ziomas, Effect of production conditions on structural properties of refractory materials, Materials Research Innovations 15 (2011) 47–52.

- [7] I.D. Katsavou, M.K. Krokida, I.C. Ziomas, Effect of production conditions on mechanical properties of bauxite refractory materials, *Ceramics - Silikaty* 53 (2009) 287–296.
- [8] A. Latella, T.L. Bruno, High-temperature young's modulus of alumina during sintering, *Journal of the American Ceramic Society* 88 (2005) 773–776.
- [9] S.S. Tomasz Sadowski, Modeling of porous ceramics response to compressive loading, *Journal of the American Ceramic Society* 86 (2003) 2218–2221.
- [10] A. Caballero, J. Requena, S. de Aza, Refractory bauxites. How processing can improve high temperature mechanical properties, *Ceramics International* 12 (1986) 155–160.
- [11] L.A. Dvaz, R. Torrecillas, F. Simonin, G. Fantozzi, Room temperature mechanical properties of high alumina refractory castables with spinel, periclase and dolomite additions, *Journal of the European Ceramic Society* 28 (2008) 2853–2858.
- [12] I.M. Low, *Ceramic Matrix Composites. Microstructure, Properties and Applications*, Woodhead Publishing, UK, 2006, p. 596.
- [13] S. Marenovic, M. Dimitrijevic, T.V. Husovic, B. Matovic, Thermal shock damage characterization of refractory composites, *Ceramics International* 34 (2008) 1925–1929.
- [14] W. Brostow, T. Datashvili, J. Geodakyan, J. Lou, Thermal and mechanical properties of EPDM/PP + thermal shock-resistant ceramic composites, *Journal of Materials Science* 46 (2011) 2445–2455.
- [15] J. Liang, Y. Wang, G. Fang, J. Han, Research on thermal shock resistance of ZrB_2 -SiC-AlN ceramics using an indentation-quench method, *Journal of Alloys and Compounds* 493 (2010) 695–698.
- [16] M.K. Krokida, C.T. Kiranoudis, Z.B. Maroulis, Viscoelastic behaviour of dehydrated products during rehydration, *Journal of Food Engineering* 40 (1999) 269–277.
- [17] M.K. Krokida, V. Oreopoulou, Z.B. Maroulis, D. Marinos-Kouris, Effect of pre-treatment on viscoelastic behaviour of potato strips, *Journal of Food Engineering* 50 (2001) 11–17.
- [18] M.K. Krokida, V.T. Karathanos, Z.B. Maroulis, Compression analysis of dehydrated agricultural products, *Drying Technology* 18 (2000) 395–408.
- [19] I.D. Katsavou, M. Krokida, I. Ziomas, Investigation of the dependence of structural and mechanical properties of cement-bonded bauxite refractories on their process conditions, *International Journal of Materials Research* 102 (2011) 1303–1311.
- [20] F.X. McConville, Engineering practice functions for easier curve fitting, *Chemical Engineering* 115 (2008) 48–51.
- [21] R.W. Rice, *Mechanical Properties of Ceramics and Composites: Grain and Particle Effects*, CRC Press, N.Y, 2000, p. 695.
- [22] Y. Pivinskii, P. Dyakin, S. Vikhman, P. Dyakin, Press-molding of high-alumina ceramic castables. 1. Compaction and properties of matrix systems based on mixed HCBS of composition: bauxite, quartz glass, and commercial alumina, *Refractories and Industrial Ceramics* 46 (2005) 220–224.
- [23] E.M. Passmore, R.M. Spriggs, T. Vasilos, Strength-grain size-porosity relations in alumina, *Journal of the American Ceramic Society* 48 (1965) 1–7.
- [24] S.B. Bonsall, P.A. Clearfield, *Refractory Compositions with Binder*, Eltra Corporation, (Morris Township, Morris County, NJ) United States, 1982.
- [25] I.I. Kabakova, et al., High-density corundum refractories of high thermal strength for high-frequency induction channel furnaces, *Refractories and Industrial Ceramics* 15 (1974) 614–617.
- [26] V.L. Balkevich, V.A. Dovbysh, The molding pressure as a factor in the high-temperature deformation properties of corundum refractories, *Refractories and Industrial Ceramics* 16 (1975) 777–779.
- [27] C. Barry Carter, M. Grant Norton, *Ceramic Materials – Science and Engineering*, Springer Science, USA, 2007, p. 716.